# Hysteresis analysis to quantify and qualify the sediment dynamics: state of the art

Simone Malutta, Masato Kobiyama, Pedro Luiz Borges Chaffe and Nadia Bernardi Bonumá

## ABSTRACT

This work is a review of the use of hysteresis to quantify sediment discharge dynamics. We reviewed 71 journal articles from the year 1953 to the present day focusing on two topics: the factors that influence hysteresis; and hysteresis quantification. The main factors influencing hysteresis are: (a) magnitude and sequence of events; (b) sediment particle size distribution; (c) basin size; and (d) land use and sediment source. Hysteresis quantification can be done using several different methods that can be grouped as: (a) hysteresis indexes; (b) statistical analysis; and (c) uncertainty analysis. Most studies were conducted in Western Europe and the USA. The studies, in general, show how the factors listed above influence the shape and patterns of hysteresis. However, the sediment dynamics are complex, and the hysteresis patterns may be linked to many other factors, such as slope and drainage systems. The quantification of hysteresis still appears, mainly with the hysteresis index and statistical analysis. Therefore, there are still many other factors that influence hysteresis patterns, as well as hysteresis rates and uncertainty analyses.

**Key words** | hysteresis, sediment, turbidity

**Simone Malutta** (corresponding author)
Federal University of Santa Catarina – Campus Joinville,
Dona Francisca Street, Joinville,
Brazil
E-mail: *simone.malutta@ufsc.br*

**Masato Kobiyama**
University of Rio Grande do Sul,
Porto Alegre,
Brazil

**Pedro Luiz Borges Chaffe**
Federal University of Santa Catarina,
Porto Alegre,
Brazil

**Nadia Bernardi Bonumá**
University of Santa Catarina,
Florianópolis,
Brazil

## INTRODUCTION

Erosion and sediment transport processes are key factors controlling water quality in rivers. Moreover, qualifying and quantifying the sediment sources may contribute to the understanding of the processes of connectivity of hillslopes to river channel (Minella & Merten 2011). Hysteresis analysis allows one to explore and evaluate the behavior of sediment transport in relation to discharge in select hydrologic events (Lloyd *et al.* 2016b). The hysteresis occurs because suspended sediment concentration (*SSC*) for a given discharge during the rising limb of the hydrograph is normally different from the falling limb due to the time lag between the discharge curve and the *SSC* curve (Mukundan *et al.* 2013). Therefore, different discharge and sediment transport processes may be identified using its hysteresis patterns (Nadal-Romero *et al.* 2008).

The hysteresis is influenced by the available amount of sediment (Gao & Josefson 2012). The magnitude and sequence of events may influence the availability of the sediment and consequently the shape of hysteresis (Asselman 1999; Hudson 2003; Rovira & Batalla 2006; Salant *et al.* 2008; Marttila & Kløve 2010). For example, if the sedimentation process is dominant the hysteresis is usually clockwise (Gao & Josefson 2012); bed and bank erosion is characterized by a counterclockwise hysteresis (Yeshaneh *et al.* 2014; Pietron et al. 2015), or an upstream section contributes to a downstream section (Asselman 1999; Salant *et al.* 2008; Smith & Dragovich 2009; Aich *et al.* 2014). The sequence of events can cause sediment exhaustion. However, other factors, such as the magnitude of the events and diameter of the particles, need to be analyzed.

The same sediment can be transported in different ways depending on the discharge magnitude (Lenzi & Marchi 2000; Salant *et al.* 2008; Landers & Sturm 2013). The particle size of the sediment will influence the transport mechanism (suspension, bearing, and skipping). In addition, sediment transport depends on the velocity of



doi: 10.2166/wst.2020.279

the water. In the headwaters, generally, the slopes are higher; in the middle course of the river, slopes decrease and velocity usually decreases accordingly, which will also lead to the deposition of this sediment, thus influencing the pattern of the hysteresis (Kronvang *et al.* 1997; Jansson 2002; Hudson 2003; Seeger *et al.* 2004; Salant *et al.* 2008; Pietron *et al.* 2015). Hysteresis patterns may also depend on the characteristics and size of the basin (Smith & Dragovich 2009).

The source of sediment can also be evaluated by using hysteresis analysis (Lefrançois *et al.* 2007; Duvert *et al.* 2010; Eaton *et al.* 2010; Minela *et al.* 2011; Hughes *et al.* 2012), such as analyzing more than one gauge station (Asselman 1999; Jansson 2002; Hudson 2003; Aich *et al.* 2014) or fingerprinting sediment (Gonzales-Inca *et al.* 2018) in catchments with different land use. There have been proposed several indexes to quantify the hysteresis patterns (e.g. Langlois *et al.* 2005; Lawler *et al.* 2006; Smith & Dragovich 2009; Aich *et al.* 2014; Lloyd *et al.* 2016a; Zuecco *et al.* 2016). Linear regression (e.g. Zabaleta *et al.* 2007; Nadal-Romero *et al.* 2008; Oeurng *et al.* 2010; Rodríguez-Blanco *et al.* 2010; Ram & Terry 2016) and multivariate statistical analysis (e.g Seeger *et al.* 2004; Zabaleta *et al.* 2007; Nadal-Romero *et al.* 2008; Oeurng *et al.* 2010; Mukundan *et al.* 2013) are commonly used to analyze the main controls on hysteresis patterns. There are still only a few studies that quantify hysteresis uncertainty (Krueger *et al.* 2009; Ziegler *et al.* 2014; Lloyd *et al.* 2016b).

In this review, we present the state of the art about the hysteresis of discharge ($Q$) and *SSC*. We analyze the four main factors that influence the hysteresis patterns: (I) the magnitude and sequence of events; (II) sediment size; (III) land use and sediment source; and (IV) basin size. We also describe the three main techniques used to analyze the hysteresis: (I) hysteresis indexes; (II) statistical analysis; and (III) uncertainty analysis.

## BIBLIOGRAPHICAL REVIEW

We have searched mainly scientific journals written in Portuguese or English. There are a few articles on conferences (IAHS Publications) and older works that are technical reports of the government of the United States which are included due to their relevance. The main studies that contributed to the *SSC*-$Q$ and turbidity-$Q$ hysteresis analysis are listed in Table S1 (supplementary material). The studies are presented in chronological order with the authors' names, basin size, country where the study was developed, year of publication, and main contributions.

In Figure 1 which shows their geographical distribution, hysteresis studies are concentrated in western Europe and the USA. There are also 27 basins studied in Russia. However, these basins were analyzed in one study only (i.e., Tananaev 2013). Table S1 and Figure 1 indicate that the hysteresis study has been carried out more in developed countries. There should be more studies, especially in the Southern Hemisphere, as there is a clear opportunity to learn about hysteresis in different climate and catchment settings.

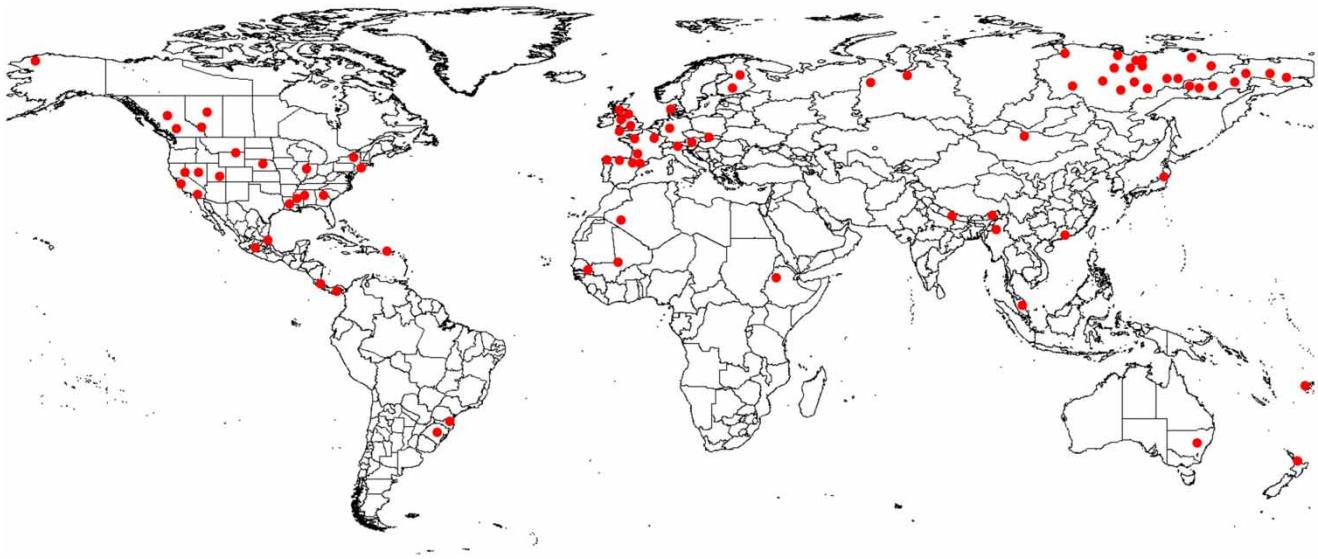

**Figure 1** | Geographical distribution of the hysteresis studies in the world (list of studies presented in Table S1 – supplementary material).

## HYSTERESIS PATTERNS

There are many types of hysteresis in the hydrological processes (such as tree cover–precipitation, water level–discharge) and their patterns depend on spatio-temporal scales (Gharari & Razavi 2018). Here, we focus only on the hysteresis between *SSC* and *Q* and between turbidity and *Q*, and the hysteresis concept is associated with the curves or loops that are formed. Leopold & Maddock (1953) were the first to analyze hysteresis between *SSC* and *Q*. During one event, sediment may not be temporally related only with the discharge (Old *et al.* 2003). The non-linearity and the hysteresis loop patterns formed by the relationship between *SSC* and *Q* or between turbidity and *Q* are widely studied and known as hysteresis (Walling & Teed 1971; Wood 1977; Klein 1984).

Williams (1989) classified those into five common patterns: (I) a single line, (II) clockwise, (III) counterclockwise, (IV) single line plus a loop, and (V) figure eight (Figure 2). Hamshaw *et al.* (2018) proposed 14 classes of hysteresis patterns based on a restricted Boltzmann machine (RBM) that allowed for sediment-discharge event dynamics including spatial scale, antecedent conditions, hydrology, and rainfall. Here we expand the list of studies of Gellis (2013) based on the patterns proposed by Williams (1989) (Table 1). When the peak of *SSC* and *Q* occurs at the same time and the rising and the falling limb of the hydrograph and sediment-graph are equal, the relation between these variables becomes linear (Type I in Figure 2). However, when there is a delay in one peak compared with the other (Type II, for example), the relation between these two variables is not linear. The *SSC-Q* relation in the rising limb is larger than in the falling limb for all the values during the event.

There are studies that have proposed *HI*s based on quantification of the curves or loops of the graphs. In general the *HI* is proposed for measuring the hysteresis loop at the different stages of the hydrograph (Lawler *et al.* 2006; Lloyd *et al.* 2016b) or the areas under the curve (Langlois *et al.* 2005).

### Single-valued line

The single-valued line occurs when the *SSC-Q* relationship is similar in the rising and falling limbs. This pattern occurs when the travel time of the discharge wave equals the time of sediment transport velocity (Yang & Lee 2018). Mossa (1989) and Hudson (2003) concluded that this type of hysteresis is formed by fine suspension sediment. It is a consequence of transport of sediment without restriction during the event, or remobilization and transport of in-channel followed by a supply from distant sources (Wood 1977; Williams 1989; Jansson 2002; Smith & Dragovich 2009; Duvert *et al.* 2010). However, the single-valued line is not common since sediment availability is exhausted during the event (Oeurng *et al.* 2010; Gao & Josefson 2012).

### Clockwise loop

The clockwise loop is the most common one (Klein 1984; Williams 1989; Jansson 2002; Hudson 2003; Rovira & Batalla 2006; Oeurng *et al.* 2010). The *SSC-Q* relation in the rising limb is larger than in the falling limb for all the values during the event. Most studies concluded that the *SSC-Q* relationship is lower in the falling limb because of the exhaustion of sediment available to be transported (Table S1). This hysteresis pattern can also be caused by the increase of the base flow during the falling limb (Walling 1974; Costa 1977; Wood 1977; Bača 2008) or be due to the fact that sediment yield areas are near river channels, and early sediment supply by the tributaries or flow paths from the source is short (de Boer & Campbell 1989; Asselman 1999; Hudson 2003; Hughes *et al.* 2012). The clockwise loop is also linked to the formation of the armoring layer before peak discharge (Williams 1989), bank erosion (Smith & Dragovich 2009), snowmelt runoff events (Gonzales-Inca *et al.* 2018), and wash load (Lenzi & Marchi 2000; Hudson 2003).

### Counterclockwise loop

A counterclockwise hysteresis pattern is formed when the peak discharge occurs before the sediment peak. The counterclockwise hysteresis is linked to: (a) flood wave traveling faster than mean flow velocity; (b) sediment wave traveling slower than the discharge wave; (c) distant sediment source, upstream tributaries, and late sediment supply by the tributaries; and (d) bed or bank erosion. Hudson (2003) identified counterclockwise hysteresis in large basins because the sediment wave traveled slower than the discharge wave. Pietron *et al.* (2015) observed that the counterclockwise hysteresis is only formed by the sediments yielded with channel erosion, not with hillslope erosion. Complementing this hypothesis, Yeshaneh *et al.* (2014) found counterclockwise hysteresis during periods when the basin was protected with vegetation and suggested that the sediment results from the erosion of the channels' bed and banks.

### Single line plus a loop

The single line plus a loop indicates that the sediment travel time is different from the flow travel time (Yang & Lee 2018).

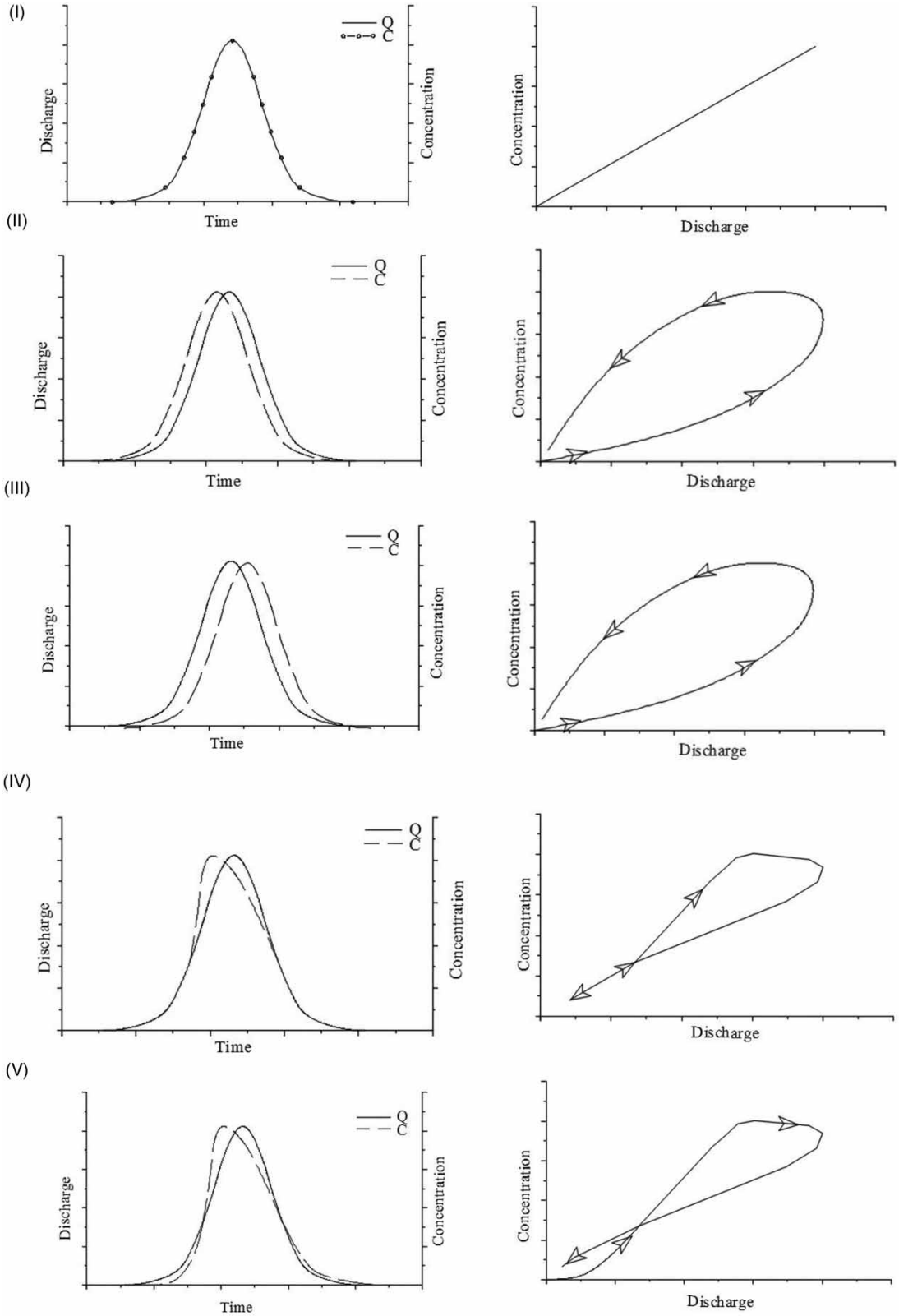


**Figure 2** | Five hysteresis patterns of sediment-discharge (after Yang & Lee (2018)).

**Table 1** | Studies for each type of hysteresis pattern

| Patterns | Cause of hysteresis | References |
|---|---|---|
| I. Single-valued line | Discharge travel time equals the sediment travel time | Yang & Lee (2018) |
| | Abundance of fine-grained sediments in the channel | Mossa (1989); Hudson (2003) |
| | Low availability of fine sediment | Walling & Webb (1982) |
| | Uninterrupted supply of sediment/remobilization and transport of in-channel followed by a supply from distant sources | Wood (1977); Williams (1989); Jansson (2002); Smith & Dragovich (2009); Duvert *et al.* (2010) |
| II. Clockwise loop or positive hysteresis | Mobilization followed by depletion of in-channel/nearby sediment sources/exhaustion effects after an initial flush of sediment | Walling (1974); Wood (1977); Costa (1977); Sidle & Campbell (1985); Kattan *et al.* (1987); Bull *et al.* (1995); Kronvang *et al.* (1997); Wang *et al.* (1998); Asselman (1999); Picouet *et al.* (2001); Lenzi & Marchi (2000); Jansson (2002); Seeger *et al.* (2004); Salant *et al.* (2008); Marttila & Kløve (2010); Smith & Dragovich (2009); Oeurng *et al.* (2010); Gao & Josefson (2012); Mukundan *et al.* (2013); Tananaev (2013); Aich *et al.* (2014) |
| | Formation of armored layer before peak discharge | Williams (1989) |
| | Bank erosion | Smith & Dragovich (2009) |
| | Increased base flow after peak discharge leading to dilution of sediment concentration | Walling (1974); Costa (1977); Wood (1977); Bača (2008) |
| | Snowmelt runoff events | Gonzales-Inca *et al.* (2018) |
| | Individual floods | Asselman (1999) |
| | Wash load (silt/clay) | Lenzi & Marchi (2000); Hudson (2003) |
| | Areas of the sediment yield are short/near-channel source/early sediment supply by the tributaries or flowpaths temporal and spatial differences between SS production and water discharge generation in small basin | de Boer & Campbell (1989); Asselman (1999); Hudson (2003); Hughes *et al.* (2012) |
| | | Sammori *et al.* (2004) |
| III. Counterclockwise loop or negative hysteresis | Floodwave traveling faster than mean flow velocity/sediment wave travels slower than the discharge wave | Heidel (1956); Marcus (1989); Williams (1989); Brasington & Richards (2000) |
| | High soil erodibility | Williams (1989) |
| | Bed and/or bank erosion | Klein (1984); Sarma (1986); Asselman (1999), Brasington & Richards (2000); Goodwin *et al.* (2003); Rinaldi *et al.* (2004); Lenzi & Marchi (2000); Hudson (2003); Fang *et al.* (2008); Marttila & Kløve (2010); Oeurng *et al.* (2010); Mukundan *et al.* (2013); Pietron *et al.* (2015) |
| | Distant sediment source/upstream tributaries/late sediment supply by the tributaries | Heidel (1956); Klein (1984); Loughran *et al.* (1986), Williams (1989); Asselman (1999); Brasington & Richards (2000); Bača (2008); Oeurng *et al.* (2010); Hughes *et al.* (2012); Gao & Josefson (2012); Mukundan *et al.* (2013); Pietron *et al.* (2015) |
| | Seasonality, lower concentrations early in the year followed by increasing sediment concentrations | Sidle & Campbell (1985); Wang *et al.* (1998) |
| | Exhaustion of sediment available due to previous event | Marttila & Kløve (2010); Oeurng *et al.* (2010); Gao & Josefson (2012) |
| | Valley slopes form the most important sediment source | Klein (1984) |
| | The distribution of non-uniform sediment yield in the basin | Williams (1989) |

(*continued*)

**Table 1** | continued

| Patterns | Cause of hysteresis | References |
|---|---|---|
| | Small events with high rainfall intensity and very dry soil conditions | Eder *et al.* (2010) |
| | Channel deposition (analyses sub-basin) | Jansson (2002) |
| | During winter freezing – river cross-sections are often fully closed with ice | Tananaev (2013) |
| | Influence of the sea tide on hysteresis | Kostaschuk *et al.* (1989) |
| | Landslide | Peart *et al.* (2005) |
| | Very high moisture and high antecedent rainfall conditions | Seeger *et al.* (2004) |
| IV. Single line plus a loop | This indicates if the sediment travel time is distinct from the flow travel time in separate runoff states | Yang & Lee (2018) |
| | Occurs under extreme dry conditions | Seeger *et al.* (2004) |
| V. Figure eight | Ice breakup | Williams (1989) |
| | Delayed contribution of sediment from sub-basins | Bača (2008); Eder *et al.* (2010) |
| | Influences of drainage system | Eder *et al.* (2010) |
| | Multiple peaks | Eder *et al.* (2010); Gao & Josefson (2012); Tananaev (2013) |
| | Sediment contribution from the streambed and its banks | Eder *et al.* (2010); Tananaev (2013) |
| VI. No hysteresis/random/ stationary | Uninterrupted supply of sediment/sediment was still available/soil surface was not protected sufficiently with vegetation cover | Bača (2008) |
| | Snowmelt and rain events | Marttila & Kløve (2010) |
| | Long events; multiple peaks; multitude of factors of sediment delivery | Nadal-Romero *et al.* (2008); Gao & Josefson (2012); Yeshaneh *et al.* (2014) |

Seeger *et al.* (2004) evidenced this hysteresis type under extremely dry conditions.

### Figure eight

The figure eight pattern can be related to: (i) the sediment deposited on the bed or banks of the channel that goes into resuspension; (ii) the time of sediment travel in upstream sub-basins; (iii) the fact that there may be an upstream storage area in the basin and, after its saturation, the contribution of the discharge and sediment downstream; and (iv) influences of the drainage system (Eder *et al.* 2010). Gao & Josefson (2012) observed this type of hysteresis in events with multiple discharge peaks.

### No hysteresis, random or stationary

There might not be any clear relationship between *SSC* and *Q* and, consequently, no typical hysteresis pattern occurs. Bača (2008) observed that there was no clear pattern when sediment remained available throughout the event (no depletion). Hysteresis without clear patterns is associated with long events with many peaks and suggesting the occurrence of several factors that contribute to the production and transport of sediment (Nadal-Romero *et al.* 2008; Gao & Josefson 2012; Yeshaneh *et al.* 2014). Marttila & Kløve (2010) found no hysteresis in rain events with snowmelt contribution.

## FACTORS CONTROLLING HYSTERESIS

### Magnitude and sequence of events

Discharge magnitude is one of the factors that cause different hysteresis patterns. The low discharge causes erosion and transports the sediment to the channel, whereas the sediment will be transported in following events with higher discharge peaks (Marttila & Kløve 2010). Therefore, the initial conditions of the sediment on the river bank and bed become important in the sediment dynamics. While in the high discharge events the sediment source may be soil erosion from the whole basin, with low discharge the sediment was from the river bed and banks

(Salant *et al.* 2008). The re-transportation of material already eroded in the channels is triggered by high discharges and generates early sediment peaks (Hudson 2003).

Sediment dynamics of the event have a common characteristic: the limitation of sediment transport in the events (Gao & Josefson 2012). Hudson (2003) suggested that there is a contribution from the sediment source of an area where there has been no exhaustion in recent events. This phenomenon was also observed by Bača (2008), who further suggested the sediment transport in one event depends on how long it takes to occur after the previous one. Erosion and deposition of sediments in the river in previous events may modify sediment dynamics (Salant *et al.* 2008). If sufficient time has passed, the soil will be eroded in a basin and there will be sediment supply again. This limitation also depends on whether the event is a 'supply-rich flood' or an 'exhaustion flood' (Rovira & Batalla 2006, Figure 3(a)). In Figure 3(b) the hydrograph and sediment-graph are schematically designed for the case where there is a sequence of events. The first and third peaks have sediment available for transport and the size of the SSC peak is larger. In the second event, there is no more sediment available and the SSC peak is smaller.

Antecedent dry days (*ADD*, Figure 4) represents the number of days between events and can be used for the analysis of the sequence of events (Mukundan *et al.* 2013). The *ADD* indicates how many days without rain there are before the event, while the antecedent precipitation index (API), which is used in most of the studies, quantifies the rain in the previous days. Even though ADD was not used in the other studies that analyzed sequences of events, it can provide important information to be included when there is a statistical analysis of sequences and sediment exhaustion.

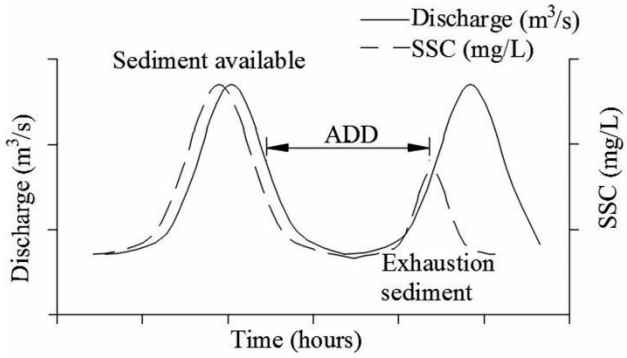


**Figure 4** | Determination of antecedent dry days (*ADD*).

## Sediment particle size distribution

Hysteresis patterns depend on the particle size distribution of the sediment available in the channel or in the basin. Hudson (2003) found that clockwise hysteresis loops occur due to a higher washload supplied by adjacent hillslopes, while in another basin, sediment transport was dominated by the bed material. As the discharge increases in the rising limb of the hydrograph, the concentration of fine sediment usually lowers in relation to the particle size of suspended sediments in source areas (Lenzi & Marchi 2000). Moreover, sand supply is quickly replenished, whereas the same does not happen in a gravel-dominated sub-basin (Salant *et al.* 2008).

Lenzi & Marchi (2000) analyzed the particle size variations of suspended material at an event. However, the studies showed variations in the relative percentage of sand and silt in transported sediment, possibly the material eroded from hillslopes and channel banks, and affect intra-storm variations in particle size.

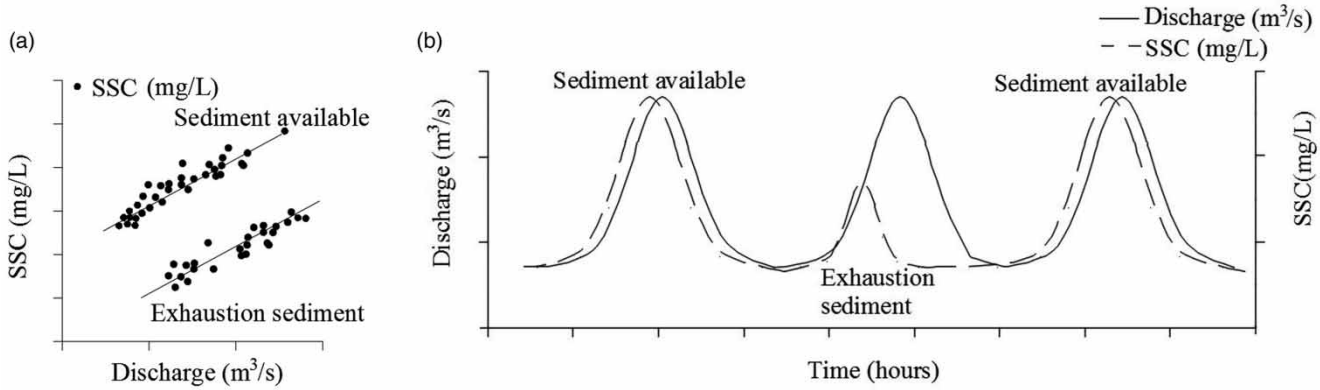


**Figure 3** | (a) Relation between suspended sediment concentration (*SSC*) and discharge for 'supply-rich floods' and 'exhaustion floods' (adapted from Rovira & Batalla (2006)). (b) Influence of the sequence of the events on hysteresis.

The particle size of the transported sediment can influence the response of optical sensors and cause interference in the construction of the turbidity-*SSC* curve (Downing 2006; Sari *et al.* 2015, 2017).

## Basin size

The hysteresis patterns depend on the characteristics and size of the basin (Smith & Dragovich 2009). In small basins (less than 10 km$^2$), the hysteresis loop is linked to factors such as soil moisture, the difference between surface and total runoff, and bank and cannel erosion (Seeger *et al.* 2004; Langlois *et al.* 2005; Lefrançois *et al.* 2007; Sadeghi *et al.* 2008; Smith & Dragovich 2009; Gao & Josefson 2012). There are no papers that establish the criteria of limits among small, medium, and large basins regarding hysteresis. There is only one indication that small basins are less than 10 km$^2$ and large drainage areas are those bigger than 100 km$^2$ (Gao & Josefson 2012). Therefore, we assume that small basins are those smaller than 10 km$^2$, and the medium and large basins are bigger than 10 km$^2$.

The hysteresis in small basins was mainly found to be controlled by the soil moisture, hydrograph separation, and bank and channel erosion (Gao & Josefson 2012). Seeger *et al.* (2004) also found that soil moisture influences hysteresis in a 2.54 km$^2$ basin. Zabaleta *et al.* (2007) investigated the hysteresis in two small basins (3 and 4.8 km$^2$) and found that sediment yield is related to total precipitation, whereas, the *SSC* is related to precipitation intensity.

Hudson (2003) identified a counterclockwise hysteresis at large basins because the sediment wave travels slower than the discharge wave. However, in larger basins it is more difficult to associate the hysteresis pattern with a single factor because there is an increasing influence of the underground and subsurface runoff, soil type, land use, and topography (Gao & Josefson 2012). In a 16 km$^2$ basin, Rodríguez-Blanco *et al.* (2010) showed that the total precipitation and the baseflow were the most relevant factors for the hydrological response, while a large part of the suspended sediment load was associated with the maximum discharge. Zabaleta *et al.* (2007) identified that in a 48 km$^2$ basin the sediment production and suspended sediment are linked neither to precipitation intensity nor to the total precipitation. While Duvert *et al.* (2010) did not find any correlation between rainfall intensity and sediment yield in a 630 km$^2$ basin due to the spatial variability of rainfall, Oeurng *et al.* (2010) found a significant correlation between precipitation and peak discharge, runoff, and sediment variables in a 1,110 km$^2$ basin. Therefore, in the case of large basins, it is essential to identify which sub-basin contributes to the water and sediment discharge and how each sub-basin influences the hysteresis.

## Land use and sediment source

Sediment yield varies according to different land uses (e.g. Duvert *et al.* 2010). Minella *et al.* (2011) evaluated factors that control hysteresis related to soil management (conventional or conservationist). The authors concluded that in the conservation period a reduction of the descending limb of the sedimentogram occurred, reducing the transport and deposit sediment in the channel and generating higher *HI*. In general, the authors pointed out that in the conventional management the *HI* was lower in the events studied – this fact being attributed to the contribution of sediment in the basin.

Table 2 shows the works that analyzed how different land use can influence the pattern of hysteresis. Gellis (2013) analyzed five basins with different land use (Table 2) and found that hysteresis patterns in each basin were associated with land use and the distance of the sediment source

**Table 2** | Characteristics of the studied basins

| Reference | Basin name | Area (km$^2$) | Slope (%) | Land use |
|---|---|---|---|---|
| Duvert *et al.* (2010) | La Cortina | 9.3 | 12 | Forest (52%), cropland (46%) |
| Duvert *et al.* (2010) | Huertitas | 3.0 | 18 | Cropland (28%), rangeland (65%), gullied (6%) |
| Duvert *et al.* (2010) | Potrerillos | 12.0 | 15 | Cropland (46%), forest (37%), grassland (23%) |
| Hughes *et al.* (2012) | Mangaotama | 2.68 | 22.5 | Forest (1%), pasture (99%) |
| Hughes *et al.* (2012) | Mangaotama* | 2.68 | 22.5 | Forest (4%), pasture (38%), pine (58%) |
| Hughes *et al.* (2012) | Whakakai | 3.11 | 23.8 | Forest (100%) |
| Gellis (2013) | Rio Icacos | 3.26 | 22.2 | Forest (100%) |
| Gellis (2013) | Quebrada Blaca | 8.42 | 33.4 | Forest (21%), pasture (54%), rural (15%), cropland (8%) |
| Gellis (2013) | Rio Caguintas | 13.7 | 33.2 | Forest (36%), pasture (27%), rural (11%), cropland (23%) |
| Gellis (2013) | Rio Piedras | 19.4 | 17.6 | Urban (77%), forest (43%) |

from the monitoring point and demonstrated that, in the forest basin (Rio Icacos), 80% of events showed clockwise hysteresis. In the basins with mixed land use (Quebrada Blanca, Rio Caguitas, and Rio Piedras) the hysteresis patterns could be both clockwise or counterclockwise. Hughes *et al.* (2012) found that in the Mangaotama basin (both before and after the integrated management), a hysteresis pattern was predominantly clockwise, suggesting that the sediment source is close to the channels. And, in the Whakakai (100% forest) the most common hysteresis pattern was counterclockwise mainly due to soil erosion from the hillslope. In the pine reforestation, the clockwise hysteresis was due to channel erosion. It was also observed that, for the same discharge magnitude, the Mangaotama basin could export up to three times more sediments than the native forest basin.

Lefrançois *et al.* (2007) studied the *SSC*-Q relationship in two basins characterized by agriculture land use. Their conclusion is that the sediment supply is defined by the number of particles that can be mobilized and that it depends on the new and deposited sediment supply. While at low discharge the sediment can be derived from the mobilization of deposited fine sediments, at high discharge it is derived from deposited coarse sediments or bank erosion. By applying the sediment fingerprinting technique with cesium-137 in order to identify suspended sediment origins, Gonzales-Inca *et al.* (2018) found that the rapid sediment mobilization during the snowmelt in a basin generated a clockwise hysteresis loop. The authors considered that cropland and stream banks were the most important sources of suspended sediments.

The hysteresis pattern results not only from the exhaustion of the sediments in the channels but also from the time of the sediment supply of the tributaries (Asselman 1999). Jansson (2002) showed that in the case of counterclockwise hysteresis, there was channel deposition between sub-basins. In another sub-basin, a rapid rising and falling discharge limb, and rapidly increasing and decreasing SSC were obtained with a small loop of hysteresis. These might result from bank erosion.

## QUANTIFICATION OF HYSTERESIS

### Hysteresis indexes

Visually it is possible to compare the pattern and size of the hysteresis. However, Langlois *et al.* (2005), Lawler *et al.* (2006), Smith & Dragovich (2009); Aich *et al.* (2014), Lloyd *et al.* (2016a), Zuecco *et al.* (2016) and so on suggested some methods to quantify the patterns, lines, curves and angles of the hysteresis (Figure 5).

The Langlois *et al.* (2005) method calculates *HI* by plotting SSC or turbidity data (dependent variable) and discharge data as an independent variable. The curves of the rising and falling limbs are generally estimated with natural logarithms and exponential equations, respectively.

The areas under the curves for the two regression equations were estimated through integration by using the minimum and maximum discharges observed in the event as the lower and higher limits, respectively. Then, the *HI* was proposed by using the ratio of these two areas:

$$HI = \frac{\int_{Q_{min}}^{Q_{max}} SSC_r}{\int_{Q_{min}}^{Q_{max}} SSC_f} \quad (1)$$

where $SSC_r$ and $SSC_f$ are the concentration of suspended sediment in rising and falling limb, respectively; and $Q_{max}$ and $Q_{min}$ are the maximum and minimum discharge in the event, respectively (Figure 5(a)).

Aich *et al.* (2014) and Zuecco *et al.* (2016) suggested the normalization of the discharge and turbidity or *SSC* data to obtain the *HI* value that is not influenced by the absolute amount of the measurements.

The index proposed by Zuecco *et al.* (2016) is basically calculated in the same way as proposed by Langlois *et al.* (2005).

In order to improve the hysteresis analysis in events, Aich *et al.* (2014) proposed to measure the maximum distance of the rising limb (*Drise*) and the falling limb (*Dfall*), and hysteresis index ($HI_A$) which is defined as the sum of *Drise* and *Dfall* (Figure 5(d)). The normalization of data allows comparison of events and the information on behavior during increase (*Drise*) and the decrease in discharge (*Dfall*). In this way, the hydrograph limb can be analyzed separately, improving the interpretation of hysteresis patterns.

The Lawler *et al.* (2006) method proposed that the *HI* should be measured at the midpoint of the discharge ($Q_{mid}$) in both the rise and fall of hysteresis (Figure 5(b)). Equation (2) determines the midpoint discharge, at which turbidity values are to be compared:

$$HI = 0.5(Q_{max} - Q_{min}) + Q_{mid} \quad (2)$$

The $TU_{RL}$ is the turbidity value at $Q_{mid}$ on the rising limb and $TU_{FL}$ is the turbidity value at $Q_{mid}$ on the falling limb of the hydrograph.

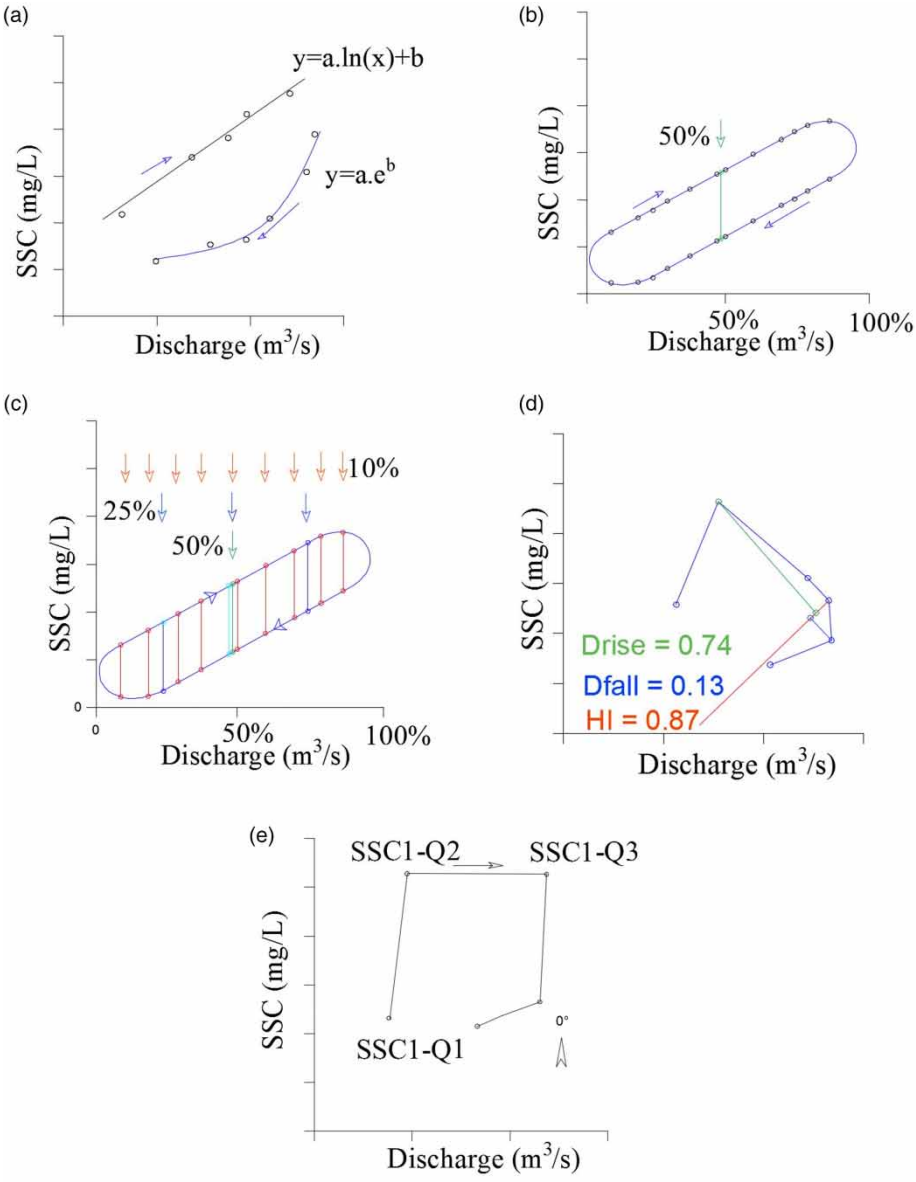


**Figure 5** | Hysteresis quantification proposals: (a) Langlois *et al.* (2005); (b) Lawler *et al.* (2006); (c) Lloyd *et al.* (2016a); (d) Aich *et al.* (2014); and (e) Smith & Dragovich (2009).

The $HI_{\min}$ of the clockwise hysteresis, i.e. $TU_{RL} > TU_{FL}$, is calculated with Equation (3), and the $HI_{\min}$ of the counter-clockwise hysteresis, i.e. $TU_{FL} > TU_{RL}$, is calculated with Equation (4):

$$HI_{\min} = \left(\left(\frac{TU_{RL}}{TU_{FL}}\right) - 1\right) \tag{3}$$

$$HI_{\min} = \left(\left(\left(\frac{-1}{\frac{TU_{RL}}{TU_{FL}}}\right)\right) + 1\right) \tag{4}$$

The *HI* proposed by Lawler *et al.* (2006) is more frequently utilized in studies, for example, Minella *et al.* (2011), Gao & Josefson (2012), and Anguilera & Melack (2018).

Based on the method of Lawler *et al.* (2006), Lloyd *et al.* (2016a) proposed a new method of calculating *HI*. This method uses the difference between turbidity or *SSC* values in the rising and falling limbs of normalized events. However, instead of calculating only the point in the $Q_{mid}$, the analysis was done at different discharge intervals (25, 10, 5, and 1%) (Figure 5(c)). The comparison of the methods showed how to characterize almost all storm sizes and

shape; the section should be calculated at least every 10% of the discharge range.

Smith & Dragovich (2009) presented another method to quantify the hysteresis patterns by applying a similarity function (*SF*). *SF* was derived based on individual line lengths and angles formed between *SSC* and *Q* (Figure 5(e)) for each sampling time (*t*).

## Statistical analysis

Table 3 shows the variables synthesized from Table S1. The variables used by most of the studies are precipitation (*P, I, Pac* and *API*), discharge ($Q_{max}$ and $Q_{med}$), and sediment or turbidity ($SSC_{max}$ and *SST*). We can highlight that Oeurng *et al.* (2010) used variables that will characterize the discharge before the event (such as $Q_{Amax}$ and $Q_{Amed}$) and that Ram & Terry (2016) used some variables to measure time, mainly turbidity dynamics (such as 'lag time'). It is also observed that only some authors used variables runoff (*R* and *C*) or base flow ($Q_A$ and $Q_{max}/Q_A$).

Most studies used the Pearson correlation matrix to identify the high linear correlations between the variables. Table 4 summarizes basin size and variables with a high correlation in various studies. After analyzing the correlations through the Pearson correlation matrix, Ram & Terry (2016) and Rodríguez-Blanco *et al.* (2010) established relationships between variables to construct a model that represents the events, giving discharge and/or turbidity and/or *SSC* as output data. Smith & Dragovich (2009) showed the correlation between the precipitation and discharge variables (*P*, *Iev*, and $Q_{max}$) with the *SF* equations.

Nadal-Romero *et al.* (2008), Oeurng *et al.* (2010), and Zabaleta *et al.* (2007) used the variables of Table 3 as input factors for analysis of principal component analysis (PCA) and factor analysis (FA, Tables 4 and 5). Seeger *et al.* (2004) used canonical analysis and not FA.

Based on the weights of the major components Mukundan *et al.* (2013) identified three important factors to generate a large variability in turbidity for each region. Therefore, PC1, PC2, and PC3 represent one (or two) subbasin of the study area. PC1 is related to the soil moisture condition of the basin (based on the weights of the ADD and $Q_{Amed}$ variables). The main component of PC2 is $NTU_{Amed}$ and the season of the year. PC3 is related to $Q_{Amed}$. The first three major components were able to explain 82% of the variability in the data.

Furthermore, Mukundan *et al.* (2013) analyzed the variables through cluster analysis. Cluster 1 showed high values of discharge and low values of turbidity; cluster 2 showed high values of high discharge and high turbidity values. Cluster 2 and 3 showed low discharge values and high turbidity values.

Analyzing the hysteresis in the basin and one sub-basin, Aich *et al.* (2014) calculated the $HI_A$, *Drise*, and *Dfall*, and correlated them with the variables of $Q_{max}$ and $SSC_{max}$ and *Pac1d, Pac7d, Pac30d, Pac60d*. The *Pac* is the accumulated precipitation before the flood (mm), e.g. *Pac1d* – 1 day. They used the Spearman coefficient (unlike most authors using the Pearson). Then, they pointed out a different behavior of the hysteresis patterns between the basin and the subbasin.

Nadal-Romero *et al.* (2008) and Oeurng *et al.* (2010) identified two PCs representing 63.5% of the data variance. In the results of Zabaleta *et al.* (2007) the variance data were smaller in two basins (Table 5).

There are a very small number of studies which carried out the statistical analysis of the variables of precipitation, discharge, turbidity, and sediment in the events. In reality, most of the studies just estimated the variables of the events, with little use of Pearson's correlation matrix, and usually not reaching the multivariate statistical analysis such as PCA and FA.

## Uncertainty analysis

The investigation of relations between methods and uncertainty can give important information on which method for each type of hysteresis pattern is better. For example, McMillan *et al.* (2012) showed benchmarking observational uncertainties for hydrology and water quality. The typical values of the relative error of discharge are ±50–100% for low flows, ±10–20% for medium or high (in-bank) flows, and a single estimate of ±40% for out-of-bank flows.

Uncertainty analysis was not presented in most of the previous studies on hysteresis analysis. There are still a few studies that analyzed the uncertainties in discharge measurements (with turbidity, sediment, or water quality parameters) with hysteresis analysis.

Based on the data presented in Lloyd *et al.* (2016a, 2016b), who used an analytical framework to evaluate uncertainty, the largest uncertainties in the *HI* were associated with the low discharge, and the largest uncertainly bounds for the loop were observed in the highest discharge.

Krueger *et al.* (2009) proposed an empirical model framework for hysteresis, where *SSC* is a function of *Q* and rate change of *Q* is proposed. The model for uncertainty analyses was the generalized likelihood uncertainty estimation (GLUE, Beven & Binley 2014).

**Table 3** | Synthesis of the variables used in statistical analysis for hysteresis studies

| | Symbol | Variables | Reference |
|---|---|---|---|
| Precipitation | $P$ | Total rainfall in the event (mm) | Seeger *et al.* (2004); Zabaleta *et al.* (2007); Nadal-Romero *et al.* (2008); Smith & Dragovich (2009); Duvert *et al.* (2010); Oeurng *et al.* (2010); Rodríguez-Blanco *et al.* (2010); Ram & Terry (2016); Sherriff *et al.* (2016) |
| | $ADD$ | Antecedent dry days | Mukundan *et al.* (2013) |
| | $I_{ev}$ | Average intensity in the event (mm/h) | Seeger *et al.* (2004); Smith & Dragovich (2009); Rodríguez-Blanco *et al.* (2010); Sherriff *et al.* (2016) |
| | $I_{max5}$ | Maximum rainfall in 5 min (mm/5 min) | Seeger *et al.* (2004); Nadal-Romero *et al.* (2008); Duvert *et al.* (2010) |
| | $I_{max10}$ | Maximum rainfall in 10 min (mm/10 min) | Zabaleta *et al.* (2007); Eder *et al.* (2010); Rodríguez-Blanco *et al.* (2010); Ram & Terry (2016); Sherriff *et al.* (2016) |
| | $I_{max30}$ | Maximum rainfall in 30 min (mm/30 min) | Seeger *et al.* (2004) |
| | $I_{maxh}$ | Maximum rainfall intensity of the flood (mm/h) | Oeurng *et al.* (2010); Ram & Terry (2016)[b]; Sherriff *et al.* (2016) |
| | $KE$ | Rainfall kinetic energy (MJ/ha) | Rodríguez-Blanco *et al.* (2010); Duvert *et al.* (2010) |
| | $Pac$, | Accumulated precipitation before the flood (mm) (Pac1d – 1 day, Pac1 h – 1 hour and thus varying the intervals) | Seeger *et al.* (2004); Zabaleta *et al.* (2007), Duvert *et al.* (2010); Oeurng *et al.* (2010); Aich *et al.* (2014); Sherriff *et al.* (2016) |
| | $API$ | Antecedent precipitation index (mm) (API1d – 1 day, API1 h – 1 hour and thus varying the intervals) | Seeger *et al.* (2004)[a]; Zabaleta *et al.* (2007); Nadal-Romero *et al.* (2008); Rodríguez-Blanco *et al.* (2010); Aich *et al.* (2014); Ram & Terry (2016); Sherriff *et al.* (2016) |
| | $t$ | Discharge duration (h) | Duvert *et al.* (2010); Oeurng *et al.* (2010); Ram & Terry (2016) |
| Discharge | $Q_{max}$ | Maximum discharge ($m^3/s$) | Lenzi & Marchi (2000); Seeger *et al.* (2004)[a]; Nadal-Romero *et al.* (2008); Salant *et al.* (2008); Smith & Dragovich (2009); Duvert *et al.* (2010); Oeurng *et al.* (2010); Rodríguez-Blanco *et al.* (2010); Gao & Josefson (2012); Aich *et al.* (2014); Sherriff *et al.* (2016) |
| | $Q_{med}$ | Mean discharge ($m^3/s$) | Hudson (2003); Seeger *et al.* (2004); Zabaleta *et al.* (2007); Oeurng *et al.* (2010); Gao & Josefson (2012); Mukundan *et al.* (2013); Ram & Terry (2016) |
| | $Q_{Amed}$ | Mean baseflow before the flood ($m^3/s$) | Oeurng *et al.* (2010) |
| | $Q_{Amax}$ | Antecedent maximum discharge | Oeurng *et al.* (2010) |
| | $Q_{base}$ | Baseflow before the flood ($m^3/s$ or l/s) | Zabaleta *et al.* (2007); Nadal-Romero *et al.* (2008); Oeurng *et al.* (2010); Rodríguez-Blanco *et al.* (2010) |
| | $Q_{max}/Q_{base}$ | | Zabaleta *et al.* (2007) |
| | $WY$ | Total water yield (mm or $m^3$) | Zabaleta *et al.* (2007); Nadal-Romero *et al.* (2008); Oeurng *et al.* (2010); Duvert *et al.* (2010); Sherriff *et al.* (2016) |
| | $R$ | Runoff | Lenzi & Marchi (2000); Nadal-Romero *et al.* (2008); Rodríguez-Blanco *et al.* (2010); Sherriff *et al.* (2016) |
| | $C$ | Coefficient of runoff | Rodríguez-Blanco *et al.* (2010); Duvert *et al.* (2010); Sherriff *et al.* (2016) |
| | $t_r$ | Time of rise (time to reach maximum discharge) | Lenzi & Marchi (2000); Oeurng *et al.* (2010) |
| Sediment and turbidity | $NTU_{max}$ | Maximum turbidity (NTU) | Ram & Terry (2016) |
| | $NTU_{med}$ | Mean turbidity (NTU) | Ram & Terry (2016) |
| | $NTU_{Amed}$ | Mean turbidity before the event (NTU) | Mukundan *et al.* (2013) |
| | $SSC_{max}$ | Maximum suspended sediment concentration (g/L) | Seeger *et al.* (2004)[a]; Zabaleta *et al.* (2007); Nadal-Romero *et al.* (2008); Salant *et al.* (2008); Oeurng *et al.* (2010); Eder *et al.* (2010); Rodríguez-Blanco *et al.* (2010); Gao & Josefson, (2012); Aich *et al.* (2014) |

(*continued*)

**Table 3** | continued

| | Symbol | Variables | Reference |
|---|---|---|---|
| | $SSC_{med}$ | Mean suspended sediment concentration (g/L) | Seeger *et al.* (2004)[a]; Nadal-Romero *et al.* (2008); Oeurng *et al.* (2010); Rodríguez-Blanco *et al.* (2010); Gao & Josefson (2012) |
| | $SSC_{Amed}$ | Mean SSC before the event (g/L) | Zabaleta *et al.* (2007) |
| | *SST* | Total suspended sediment yield (kg, ton, or Mg) | Zabaleta *et al.* (2007); Nadal-Romero *et al.* (2008); Oeurng *et al.* (2010); Eder *et al.* (2010); Rodríguez-Blanco *et al.* (2010); Gao & Josefson (2012) |
| | $NTU_d$ | Turbidity response duration | Ram & Terry (2016) |
| | *LagR-NTU* | Lag time from rainfall start to maximum turbidity | Ram & Terry (2016) |
| | $LagRI_{max}$-*NTU* | Lag time from maximum rainfall intensity to maximum turbidity | Ram & Terry (2016) |
| | *Season* | Season of year | Mukundan *et al.* (2013) |

[a]The time interval of measurement was 5 minutes and 30 minutes.
[b]In this study, the authors had two rainfall measurement stations, with which the maximum intensity estimation was done.

**Table 4** | Variables with high linear correlation

| Reference | Variable | High linear correlations | Basin area (km²) |
|---|---|---|---|
| Nadal-Romero *et al.* (2008) | *P* | $Q_{max}$, *R*, $SSC_{max}$, *STT* and *WY* | 0.45 |
| | *WY*, *R* and $Q_{max}$ | *P*, $Imax_5$ | |
| | $SSC_{max}$ and *SST* | $Q_{max}$, *P*, *R* | |
| Oeurng *et al.* (2010) | *P* | $Q_{med}$, $Q_{max}$, $SSC_{max}$, *STT* and *WY* | 1,110 |
| | $Q_{med}$, $Q_{max}$ | *P*, $Q_{Amed}$, *Qbase* | |
| | $SSC_{max}$ and *SST* | *P*, $I_{maxh}$, *R*, *Qmed*, $Q_{max}$. | |
| Zabaleta *et al.* (2007) | *P* | $Q_{med}$, *WY*, $Q_{max}$ | 4.8 |
| | *SST* | *P*, $SSC_{med}$, $SSC_{max}$ | |
| | *SST* | *P* | 3 |
| | $SSC_{med}$ and $SSC_{max}$ | $I_{max10}$ | |
| | $Q_{med}$, $Q_{max}$ and *WY* | *API1d*, *API1 h*, | 48 |
| | *SST* | *API1d*, *API1 h*, | |
| Rodríguez-Blanco *et al.* (2010) | $Q_{max}$, *R*, *C* | *P*, *Ke*, $Q_b$, | 16 |
| | *ST* | *P*, *Ke*, $Q_{max}$, *R*, *C* | |
| | $SSC_{max}$ | *P*, *Ke*, $Q_{max}$ | |
| | $SSC_{med}$ | *P*, $Q_{max}$ | |
| Ram & Terry (2016) | $NTU_d$ | *P*, *Iev*, $D_{max}$ | 9.3 |
| | $NTU_{med}$ | *P*, $D_{max}$, $I_{ev}$ $I_{max10}$ | |
| | $NTU_{max}$ | *P*, $D_{max}$, $I_{ev}$, $I_{max10}$ | |

**Table 5** | Summary of study basins areas and the results of PCA and FA

| Reference | Area (km²) | Variable | Variance |
|---|---|---|---|
| Mukundan *et al.* (2013) | 493 | *ADD* $Q_{Amed}$ $NTU_{Amed}$ *Season of year* $Q_{Amed}$ | 82% |
| Nadal-Romero *et al.* (2008) | 0.45 | *WY*, $Q_{max}$, $SSC_{max}$, *SST*, *P* | 44% |
| | | *R*, $I_{max5}$, *API* | 19.5% |
| Oeurng *et al.* (2010) | 1,110 | *Td*, $Q_{med}$, *Qmax*, *P*, *WY*, *SST* | 46.7% |
| | | *If*, $SSC_{med}$, $SSC_{max}$, $I_{maxh}$ | 16.83% |
| Zabaleta *et al.* (2007) | 4.8 | $I_{ev}$, $Imax_5$, $SSC_{med}$, $SSC_{max}$, $Q_{max}/Qb$ | 29% |
| | | *P*, *WY*, *Qmed* | 23% |
| | 3 | $Q_{med}$, *Qmax*, *Qt*, *SSt* | 33% |
| | | *Iev*, $Imax_5$, *SSCmax*, $SSC_{med}$ | 28% |
| | 48 | $Q_{med}$, $Q_{med}$, *WY*, *API1d*, *API1 h* | 47% |
| | | $SSC_{med}$, $SSC_{med}$ | 22% |
| Seeger *et al.* (2004) | 2.84 | *P*, *APd3*, *SWC*[a] | 78% |
| | | *P*, *APd3*, *SWC*[a] | 21% |

[a]*SWC*, soil water content.

Thus, it is necessary to pay attention to these data as well as the process of obtaining the data and estimating their uncertainty. There was a close relation between turbidity and *SSC* (Navratil *et al.* 2011), which allows the use of turbidity as an indirect measure of *SSC*. However, it must be noted that there are several factors of uncertainty associated with this relation. The interference caused by the

sediment was a function of the *SSC*, the particle size, shape, roughness, color, and mineralogy composition (Downing 2006; Sari *et al.* 2015, 2017).

For example, the optical sensor measures mA or mV, which is transformed into turbidity by one or more equations. Another equation transforms the turbidity into *SSC*, which consequently creates a number of factors influencing the final value of *SSC*. If a sensor could be developed for direct measurement of *SSC*, these types of uncertainty or errors could be reduced. There are some studies that do this conversion directly (Brasington & Richards 2000, for example).

As mentioned above, the particle size also interferes with the optical sensor response. Harmel & Smith (2006) carried out streamflow measurement, sample collection, sample preservation/storage, and laboratory analysis during the storm events. Then, they demonstrated that the cumulative probable uncertainty during the events varied from 3% (the best case) to 117% (the worst case). This type of interference is not often quantified in scientific studies.

Ziegler *et al.* (2014) studied hysteresis with uncertainty in the turbidity-*SSC*, and also the problems with the limitations related to the turbidity sensor. They reported an interval in their annual estimates (underestimated by 38–43% and overestimated by 28–33%).

## FINAL REMARKS

In a review of 71 papers we identified the most significant factors influencing sediment-discharge hysteresis: the magnitude and sequence of events; the sediment particle size distribution; land use and sediment source; and the basin area. The sequence of events can cause sediment exhaustion; with less sediment available the hysteresis loop may get smaller. Small particle size sediments are replenished faster because they can be transported by low discharge also. Therefore, there is a binding of at least three factors (magnitude, sequence, and diameter of the particles) to be analyzed. There is still a need to systematize ways of measuring the magnitude of discharge, mainly because the study basins have different sizes and varying magnitudes of discharge.

Land use influences the amount of sediment produced, but those hypotheses related to land use were not fully tested. The basin size factor influences the hysteresis due to the different behaviors of the hydrological and sediment processes in small and large basins. Studies typically use statistical analysis to analyze which processes most influence hysteresis. In small basins the factors that influence it are soil moisture and runoff. There seems to be no consensus on quantifying hysteresis in medium and large basins. But overall, studies show that for large basins the precipitation, discharge, and sediment variables control hysteresis.

Three main techniques were identified that can be used to analyze the hysteresis quantitatively: (a) hysteresis indexes; (b) statistical analysis (simple or multivariate); and (c) uncertainty analysis. The *HI* is very commonly used. It is based on the difference in sediment concentration or turbidity in the rise and fall of the hydrograph in the different curves and quickly shows (due to the simplicity of the calculation) the measurement of the two limbs. Statistical analysis of hydrological and sedimentological variables turned out to be a tool for analyzing the processes in the events and not a quantification of the hysteresis itself. Most studies divide their samples into small and large basins and use correlation statistics to explore what processes are more significant in each case.

Even though the area of the uncertainty of estimation in hydrology has been increasingly applied over the past 20 years, there are still a few studies that used it in hysteresis analysis. Furthermore, there are studies that include only sediment uncertainty and limitations on the analysis of events on a temporal scale (annual or monthly among others. Hence, there are opportunities for further exploration of hysteresis and uncertainty analysis.

## SUPPLEMENTARY MATERIAL

The Supplementary Material for this paper is available online at https://dx.doi.org/10.2166/wst.2020.279.

## REFERENCES

Aich, V., Zimmermann, A. & Elsenbeer, H. 2014 Quantification and interpretation of suspended-sediment discharge hysteresis patterns: how much data do we need? *Catena* **122**, 120–129. 10.1016/j.catena.2014.06.020.

Anguilera, R. & Melack, J. M. 2018 Concentration-discharge responses to storm events in coastal California watersheds. *Water Resources Research* **54**, 407–424. 10.1002/2017WR021578.

Asselman, N. E. M. 1999 Suspended sediment dynamics in a large drainage basin: the River Rhine. *Hydrological Processes* **13**, 1437–1450.

Bača, P. 2008 Hysteresis effect in suspended sediment concentration in the Rybárik basin, Slovakia. *Hydrological Sciences Journal* **53** (1), 224–235. 10.1623/hysj.53.1.224.

Beven, K. & Binley, A. 2014 GLUE: 20 years on. *Hydrological Processes* **28**, 5897–5918. 10.1002/hyp.10082.

Brasington, J. & Richards, K. 2000 Turbidity and suspended sediment dynamics in small catchments in the Nepal Middle Hills. *Hydrological Processes* **14**, 2559–2574. 10.1002/1099-1085(20001015)14:14<2559::AID-HYP114>3.0.CO;2-E.

Bull, L. J., Lawler, D. M., Leeks, G. J. L. & Marks, S. 1995 Downstream changes in suspended sediment fluxes in the River Severn, UK. In: *Effects of Scale on Interpretation and Management of Sediment and Water Quality, Proceedings of the Boulder Symposium*, July 1995. International Association of Hydrological Sciences Publication, Vol. 226, pp. 27–37.

Costa, J. E. 1977 Sediment concentration and duration in stream channels. *Journal of Soil and Water Conservation* **32** (4), 168–170.

de Boer, D. H. & Campbell, I. A. 1989 Spatial scale dependence of sediment dynamics in a semi-arid badland drainage basin. *Catena* **16**, 277–290.

Downing, J. 2006 Twenty-five years with OBS sensors: the good, the bad, and the ugly. *Continental Shelf Research* **26**, 2299–2318. 10.1016/j.csr.2006.07.018.

Duvert, C., Gratiot, N., Evrard, O., Navratil, O., Némery, J., Prat, C. & Esteves, M. 2010 Drivers of erosion and suspended sediment transport in three headwater catchments. *Geomorphology* **123**, 243–256. 10.1016/j.geomorph.2010.07.016.

Eaton, B. C., Moore, R. D. & Giles, T. R. 2010 Forest fire, bank strength and channel instability: the 'unusual' response of Fishtrap Creek, British Columbia. *Earth Surface Processes and Landforms* **35**, 1167–1183. 10.1002/esp.1946.

Eder, A., Strauss, P., Krueger, T. & Quinton, J. N. 2010 Comparative calculation of suspended sediment loads with respect to hysteresis effects (in the Petzenkirchen catchment, Austria. *Journal of Hydrology* **389**, 168–176. 10.1016/j.jhydrol.2010.05.043.

Fang, H. Y., Cai, Q. G., Chen, H. & Li, Q. Y. 2008 Temporal changes in suspended sediment transport in a gullied loess basin: the lower Chabagou Creek on the Loess Plateau in China. *Earth Surface Processes and Landforms* **33**, 1977–1992. 10.1002/esp.1649.

Gao, P. & Josefson, M. 2012 Event-based suspended sediment dynamics in a central New York watershed. *Geomorphology* **139–140**, 425–437. 10.1016/j.geomorph.2011.11.007.

Gellis, A. C. 2013 Factors influencing storm-generated suspended-sediment concentrations and loads in four basins of contrasting land use, humid-tropical Puerto Rico. *Catena* **104**, 39–57. 10.1016/j.catena.2012.10.018.

Gharari, S. H. & Razavi, S. 2018 Hysteresis in hydrology and hydrological modeling: memory, path-dependency, or missing physics? *Journal of Hydrology* **556**, 500–519. 10.1016/j.jhydrol.2018.06.037.

Gonzales-Inca, C., Valkama, P., Lill, J. O., Slotte, J., Heiteharju, E. & Uusitalo, R. 2018 Spatial modeling of sediment transfer and identification of sediment sources during snowmelt in an agricultural watershed in boreal climate. *Science of the Total Environment* **612**, 303–312. 10.1016/j.scitotenv.2017.08.142.

Goodwin, T. H., Young, A. R., Holmes, G. R., Old, G. H., Hewitt, N., Leeks, G. J. L., Packman, J. C. & Smith, B. P. G. 2003 The temporal and spatial variability of sediment transport and yields within the Bradford Beck catchment, West Yorkshire. *The Science of the Total Environment* **3114–3116**, 475–494. 10.1016/S0048-9697(03)00069-X.

Hamshaw, S. D., Dewoolkar, M., Schroth, A. W., Wemple, B. C. & Rizzo, D. M. 2018 A new machine-learning approach for classifying hysteresis in suspended-sediment discharge relationships using high-frequency monitoring data. *Water Resource Research* **54** (6), 4040–4058. 10.1029/2017WR022238.

Harmel, R. D. & Smith, P. 2006 Consideration of measurement uncertainty in the evaluation of goodness-of-fit in hydrologic and water quality modeling. *Journal of Hydrology* **337**, 326–336. 10.1016/j.jhydrol.2007.01.043.

Heidel, S. G. 1956 The progressive lag of sediment concentration with flood waves. *American Geophysical Union Transactions* **37**, 56–66.

Hudson, P. F. 2003 Event sequence and sediment exhaustion in the lower Panuco Basin, México. *Catena* **52**, 57–76. 10.1016/S0341-8162(02)00145-5.

Hughes, A. O., Quinn, J. M. & McKergow, L. A. 2012 Land use influences on suspended sediment yields and event sediment dynamics within two headwater catchments, Waikato, New Zealand. *New Zealand Journal of Marine and Freshwater Research* **46** (3), 315–333. 10.1080/00288330.2012.661745.

Jansson, M. B. 2002 Determining sediment source areas in a tropical river basin, Costa Rica. *Catena* **47**, 63–84. 10.1016/S0341-8162(01)00173-4.

Kattan, Z., Ga, J. Y. & Probst, J. L. 1987 Suspended sediment load and mechanical erosion in the Senegal basin – estimation of the surface runoff concentration and relative contributions of channel and slope erosion. *Journal of Hydrology* **92**, 59–76. 10.1016/0022-1694(87)90089-8.

Klein, M. 1984 Anti clockwise hysteresis in suspended sediment concentration during individual storms. *Catena* **11**, 251–257. 10.1016/0341-8162(84)90014-6.

Kostaschuk, R. A., Luternauer, J. L. & Church, M. A. 1989 Suspended sediment hysteresis in a salt-wedge estuary: Fraser River, Canada. *Marine Geology* **87**, 273–285.

Kronvang, B., Laubel, A. & Grant, R. 1997 Suspended sediment and particulate phosphorus transport and delivery pathways in an arable catchment, Gelbák stream, Denmark. *Hydrological Processes* **11**, 627–642. 10.1002/(SICI)1099-1085(199705)11:6<627::AID-HYP481>3.0.CO;2-E.

Krueger, T., Quinton, J. N., Freer, J., Macleod, C. J. A., Bilotta, G. S., Brazier, R. E., Butler, P. & Haygarth, P. M. 2009 Uncertainties in data and models to describe event dynamics of agricultural sediment and phosphorus transfer. *Journal of Environmental Quality* **38** (3), 1137–1148. 10.2134/jeq2008.0179.

Landers, M. N. & Sturm, T. W. 2013 Hysteresis in suspended sediment to turbidity relations due to changing particle size

distributions. *Water Resources Research* **49** (9), 5487–5500. doi.org/10.1002/wrcr.20394.

Langlois, J. L., Johnson, D. W. & Mehuys, G. R. 2005 Suspended sediment dynamics associated with snowmelt runoff in a small mountain stream of Lake Tahoe (Nevada). *Hydrological Processes* **19**, 3569–3580. 10.1002/hyp.5844.

Lawler, D. M., Petts, G. E., Foster, I. D. L. & Harper, S. 2006 Turbidity dynamics during spring storm events in an urban headwater river system: the Upper Tame, West Midlands, UK. *The Science of the Total Environment* **360**, 109–126. 10.1016/j.scitotenv.2005.08.032.

Lefrançois, J., Grimaldi, C., Gascuel-Odoux, C. & Gilliet, N. 2007 Suspended sediment and discharge relationships to identify bank degradation as a main sediment source on small agricultural catchments. *Hydrological Processes* **21** (21), 2923–2933. 10.1002/hyp.6509.

Lenzi, M. A. & Marchi, L. 2000 Suspended sediment load during floods in a small stream of the Dolomites (northeastern Italy). *Catena* **39**, 267–282. 10.1016/S0341-8162(00)00079-5.

Leopold, L. B. & Maddock, T. 1953 The hydraulic geometry of stream channels and some physiographic implications. *Geological Survey Professional Paper* 252. 10.3133/pp252.

Lloyd, C. E. M., Freer, J. E., Johnes, P. J. & Collins, A. L. 2016a Technical note: testing an improved index for analysing storm discharge–concentration hysteresis. *Hydrology and Earth System Sciences* **20**, 625–632. 10.5194/hess-20-625-2016.

Lloyd, C. E. M., Freeer, J. E., Johnes, P. J. & Collins, A. L. 2016b Using hysteresis analysis of high-resolution water quality monitoring data, including uncertainty, to infer controls on nutrient and sediment transfer in catchments. *Science of the Total Environment* **543**, 388–404. 10.1016/j.scitotenv.2015.11.028.

Loughran, R. J., Campbell, B. L. & Elliott, G. L. 1986 Sediment dynamics in a partially cultivated catchment in New South Wales, Australia. *Journal of Hydrology* **83**, 285–297.

Marcus, A. W. 1989 Lag-time routing of suspended sediment concentrations during unsteady flow. *Geological Society of America Bulletin* **101**, 644–651.

Marttila, H. & Kløve, B. 2010 Dynamics of erosion and suspended sediment transport from drained peatland forestry. *Journal of Hydrology* **388**, 414–425. 10.1016/j.jhydrol.2010.05.026.

McMillan, H., Krueger, T. & Freer, J. 2012 Benchmarking observational uncertainties for hydrology: rainfall, river discharge and water quality. *Hydrological Processes* **26**, 4078–4111. 10.1002/hyp.9384.

Minella, J. P. G. & Merten, G. H. 2011 Monitoramento de bacias hidrográficas para identificar fontes de sedimentos em suspensão. *Revista Ciência Rural* **41** (3), 424–432. 10.1590/S0103-84782011000300010.

Minella, J. P. G., Merten, G. H. & Magnago, F. P. 2011 Análise qualitativa e quantitativa da histerese entre vazão e concentração de sedimentos durante eventos hidrológicos (Qualitative and quantitative analysis of hysteresis between discharge and sediment concentration during hydrological events). *Revista Brasileira de Engenharia Agrícola e Ambiental (Journal of the Brazilian Association of Agricultural and Environmental Engineering)* **15** (12), 1306–1313. 10.1590/S1415-43662011001200013.

Mossa, J. 1989 Hysteresis and nonlinearity of discharge-sediment relationships in the Atchafalaya and lower Mississippi rivers. In: *Sediment and the Environment, Proceedings of the Baltimore Symposium*. Vol. 184, IAHS Publications, Australia.

Mukundan, R., Pierson, D. C., Schneiderman, E. M., ODonnell, D. M. & Pradhnang, S. M. 2013 Factors affecting storm event turbidity in a New York City water supply stream. *Catena* **207**, 80–88. 10.1016/j.catena.2013.02.002.

Nadal-Romero, E., Regüés, D. & Latron, J. 2008 Relationships among rainfall, runoff, and suspended sediment. *Catena* **74**, 127–136. 0.1016/j.catena.2008.03.014.

Navratil, O., Esteves, M., Legout, C., Grtiot, N., Nemery, J., Willmore, S. & Grangeon, T. 2011 Global uncertainty analysis of suspended sediment monitoring using turbidimeter in a small mountainous river catchment. *Journal of Hydrology* **398** (3–4), 246–259. 10.1016/j.jhydrol.2010.12.025.

Oeurng, C., Sauvage, S. & Sánchez-Pérez, J.-M. 2010 Dynamics of suspended sediment transport and yield in a large agricultural catchment, southwest France. *Earth Surface Processes and Landforms* **35**, 1289–1301. 10.1002/esp.1971.

Old, G. H., Leeks, G. J. L., Packman, J. C., Smith, B. P. G., Lewis, S., Hewitt, E. J., Holmes, M. & Young, A. 2003 The impact of a convectional summer rainfall event on river flow and fine sediment transport in a highly urbanised catchment: Bradford, West Yorkshire. *Science of the Total Environment* **314–316**, 495–512.

Peart, M. R., Ruse, M. E. & Fok, L. 2005 Sediment delivery from a landslide to stream in drainage basin in Hong Kong. In: *Geomorphological Processes and Human Impacts in River Basins (Proceedings of the International Conference Held at Solsona, Catalonia, Spain)*. Vol. 299, IAHS Publications.

Picouet, C., Hingray, B. & Olivry, J. C. 2001 Empirical and conceptual modelling of the suspended sediment dynamics in a large tropical African river: the Upper Niger River basin. *Journal of Hydrology* **250**, 19–39. 10.1016/S0022-1694(01)00407-3.

Pietron, J., Jarjo, J., Romanchenko, A. & Chalov, S. R. 2015 Model analyses of the contribution of in-channel processes to sediment concentration hysteresis loops. *Journal of Hydrology* **527**, 576–589. 10.1016/j.jhydrol.2015.05.009.

Ram, A. F. & Terry, J. P. 2016 Stream turbidity responses to storm events in a pristine rainforest watershed on the coral coast of southern Fiji. *International Journal of Sediment Research* **31**, 279–290. 10.1016/j.ijsrc.2016.07.002.

Rinaldi, M., Casagli, N., Dapporto, S. & Gargini, A. 2004 Monitoring and modeling of pore water pressure changes and riverbank stability during flow events. *Earth Surface Processes and Landforms* **29** (2), 237–254. 10.1002/esp.1042.

Rodríguez-Blanco, M. L., Taboada-Castro, M. M. & Taboada-Castro, M. T. 2010 Factors controlling hydro-sedimentary response during runoff events in a rural catchment in the humid Spanish zone. *Catena* **82**, 206–217. 10.1016/j.catena.2010.06.007.

Rovira, A. & Batalla, R. J. 2006 Temporal distribution of suspended sediment transport in a Mediterranean basin: the

Lower Tordera (NE SPAIN). *Geomorphology* **79**, 58–71. 10.1016/j.geomorph.2005.09.016.

Sadeghi, S. H. R., Mizuyama, T., Miyata, S., Gomi, T., Kosugi, K., Fukushima, T., Mizugaki, S. & Onda, Y. 2008 Determinant factors of sediment graphs and rating loops in a reforested watershed. *Journal of Hydrology* **356**, 271–282. 10.1016/j.geoderma.2007.11.008.

Salant, N. L., Hassan, M. A. & Alonso, C. V. 2008 Suspended sediment dynamics at high and low storm flows in two small watersheds. *Hydrological Processes* **22**, 1573–1587. 10.1002/hyp.6743.

Sammori, T., Yusop, Z., Kasran, B., Noguchi, S. & Tani, M. S. 2004 Suspended solids discharge fom a small forested basin in the humid tropics. *Hydrological Processes* **18**, 721–738. 10.1002/hyp.1361.

Sari, V., Castro, N. M. R. & Kobiyama, M. 2015 Estimativa da concentração de sedimentos suspensos com sensores ópticos: revisão. *Revista Brasileira de Recursos Hídricos* **20–4**, 816–836.

Sari, V., Pereira, M. A., Castro, N. M. R. & Kobiyama, M. 2017 Efeitos do tamanho da partícula e da concentração de sedimentos suspensos sobre a turbidez. *Engenharia Sanitaria e Ambiental* **22-2**, 213–219. 10.1590/S1413-41522016144228.

Sarma, J. N. 1986 Sediment transport in the Burhi Dihing River, India. In: *Drainage Basin Sediment Delivery* (R. F. Hadley, ed.). IAHS Publications 159, pp. 199–215.

Seeger, M., Errea, M. P., Beguería, S., Arnáez, J., Martí, C. & García-Ruiz, J. M. 2004 Catchment soil moisture and rainfall characteristics as determinant factors for discharge/suspended sediment hysteretic loops in a small headwater catchment in the Spanish Pyrenees. *Journal of Hydrology* **288**, 299–311. 10.1016/j.jhydrol.2003.10.012.

Sherriff, S. C., Rowan, J. S., Fenton, O., Jordan, P., Melland, A. R. & Ó hUallacháin, D. 2016 Storm event suspended sediment-discharge hysteresis and controls in agricultural watersheds: implications for watershed scale sediment management. *Environmental Science & Technology* **50** (4), 1769–1778. 10.1021/acs.est.5b04573.

Sidle, R. C. & Campbell, A. J. 1985 Patterns of suspended-sediment transport in a coastal Alaska stream. *Journal of the American Water Resources Association* **21**, 909–917. 10.1111/j.1752-1688.1985.tb00186.x.

Smith, H. G. & Dragovich, D. 2009 Interpreting sediment delivery processes using suspended sediment-discharge hysteresis patterns from nested upland catchments, south-eastern Australia. *Hydrological Processes* **23** (17), 2415–2426. 10.1002/hyp.7357.

Tananaev, N. 2013 Hysteresis effects of suspended sediment transport in relation to geomorphic conditions and dominant sediment sources in medium and large rivers of Russian Arctic. *Hydrology Research* **46** (6), 232–243. 10.2166/nh.2013.199.

Walling, D. E. 1974 Suspended sediment and solute yields from a small catchment prior to urbanization. In: *Fluvial Processes in Instrumented Watersheds* (K. J. Gregory & D. E. Walling, eds). Institute of British Geographers Special Publication 6, IBG, London, UK, pp. 169–192.

Walling, D. E. & Teed, A. 1971 A simple pumping sampler for research into suspended sediment transport in small catchments. *Journal of Hydrology* **13**, 325–337. 10.1016/0022-1694(71)90251-4.

Walling, D. E. & Webb, B. W. 1982 Sediment availability and the prediction of stormperiod sediment yields. *International Association of Hydrological Sciences Publication* **137**, 327–337.

Wang, Y., Ren, M. & Syvitski, J. P. M. 1998 Sediment transport and terrigenous flux. In: *The Sea. Volume 10, The Global Coastal Ocean* (K. H. Brink & A. R. Robinson, eds). Wiley, New York, USA, pp. 253–292.

Williams, G. P. 1989 Sediment concentration versus water discharge during single hydrologic events in rivers. *Journal of Hydrology* **111**, 89–106. 10.1016/0022-1694(89)90254-0.

Wood, P. A. 1977 Controls of variation in suspended sediment concentration in the River Rother, West Sussex, England. *Sedimentology* **24**, 437–445. doi.org/10.1111/j.1365-3091.1977.tb00131.x.

Yang, C. & Lee, K. Y. 2018 Analysis of flow-sediment rating curve hysteresis based on flow and sediment travel time estimations. *International Journal of Sediment Research* **33**, 171–182. 10.1016/j.ijsrc.2017.10.003.

Yeshaneh, E., Eder, A. & Blöschl, G. 2014 Temporal variation of suspended sediment transport in the Koga catchment, North Western Ethiopia and environmental implications. *Hydrological Processes* **28**, 5972–5984. 10.1002/hyp.10090.

Zabaleta, A., Martínez, M., Uriarte, J. A. & Antigüedad, I. 2007 Factors controlling suspended sediment yield during runoff events in small head water catchments of the Basque Country. *Catena* **71**, 179–190. 10.1016/j.catena.2006.06.007.

Ziegler, A. D., Benner, G. S., Tantasirin, C., Wood, S. H., Sutherland, R. A., Sidle, R. C., Jachowski, N., Nullet, M. A., Xi Xi, L., Snidvongs, A., Giambelluca, T. W. & Fox, J. M. 2014 Turbidity-based sediment monitoring in northern Thailand: hysteresis, variability, and uncertainty. *Journal of Hydrology* **519**, 2020–2039. 10.1016/j.jhydrol.2014.09.010.

Zuecco, G., Penna, D., Borga, M. & van Meerveld, H. J. 2016 A versatile index to characterize hysteresis between hydrological variables at the runoff event timescale. *Hydrological Processes* **30**, 1449–1466. 10.1002/hyp.10681.

First received 30 January 2020; accepted in revised form 29 May 2020. Available online 12 June 2020